SMGroup

SM Journal of Minimally Invasive Surgery

Research Article

Hybrid Navigation Information System for Minimally Invasive Surgery -Phase I: Offline Sensors Registration

Uddhav Bhattarai and Ali T Alouani*

Department of Electrical and Computer Engineering, Tennessee Technological University, USA

Article Information

Received date: Sep 07, 2018
Accepted date: Nov 12, 2018
Published date: Nov 15, 2018

***Corresponding author**

Ali T. Alouani, Department of Electrical and Computer Engineering, Tennessee Technological University, USA;
Email: mailto:aalouani@tntech.edu

Keywords Multisensor system, Sensor fusion, Calibration, Computer assisted surgery, biomedical signal processing, and Image guided treatment

Abstract

Current minimally invasive surgery (MIS) technology, although advantageous compared to open cavity surgery in many aspects, has limitations that prevents its use for general purpose MIS. This is due to reduced dexterity, cost, and required complex training of the currently practiced technology. The main challenges in reducing cost and amount of training is to have an accurate inner body navigation advisory system to help guide the surgeon to reach the surgery location.

As a first step in making minimally invasive surgery affordable and more users friendly, quality images inside the patient as well as the surgical tool location should be provided automatically and accurately in real time in a common reference frame.

The objective of this paper is to build a platform to accomplish this goal. It is shown that a set of three heterogeneous asynchronous sensors is a minimum requirement for navigation inside the human body.

The sensors have different data rate, different reference frames, and independent time clocks. A prerequisite for successful information fusion is to represent all the sensors data in a common reference frame. The focus of this paper is on off line calibration of the three sensors, i.e. before the surgical device is inserted in the human body. This is a pre-requisite for real time navigation inside the human body.

The proposed off-line sensor registration technique was tested using experimental laboratory data. The result of calibration was promising with an average error of 0.1081mm and 0.0872mm along the x and y directions, respectively, in the 2D camera image.

Introduction

Minimally Invasive Surgery (MIS) does not require opening the patient body to perform surgical procedure.

This method has distinct merits of faster recovery; shorter hospital stays, less pain, and decreased scarring. However, restricted visualization of operative site, minimal accessibility, and reduced dexterity has increased the challenges of its implementation. Image Guided Surgery (IGS) during MIS will help to solve such problems and improve safety and accuracy to significant level [1].

Computed Tomography (CT)/Magnetic Resonance Imaging (MRI) provide high quality images of the inside of the patient body [2]. Surgical planning may involve getting insight of patient anatomy, analyzing it, and developing the effective treatment approach [2]. The preoperative images expire within minutes because the intraoperative environment changes continuously due to manipulation by surgeon or organ movement. Hence an intraoperative imaging system with navigation mechanism is required to provide the real-time changes in the map provided by the preoperative data [2]. The process of registration/calibration is needed to transform a point/collection of points from one coordinate frame to another. Thus, one can acquire all the data in a single coordinate frame for the purpose of data fusion in order to achieve more accurate and informative results than what single sensor can provide.

Spatial calibration deals with determination of spatial transformation parameters between the coordinate frames while the temporal calibration is for time synchronization of multiple asynchronous sensor data. Temporal calibration is beyond the scope of this paper, and further reading can be found in [3-5]. The surface based spatial registration between preoperative CT and intraoperative ultrasound in [6]; LapAssistent [7] was carried out by using Iterative Closest Point (ICP) algorithm. ICP suffers from being trapped in local minima unless a good initial guess is provided. In addition, it requires computation of closest point pair for operation so it has limited computational speed. Furthermore, the reported accuracy in [7] doesn't provide reliability for clinical application in human body.

The use of Hand-Eye calibration for rigid registration among robotic arm, tracking devices (EMTS/Optical Tracking System (OTS)) and imaging devices (Endoscope/Laparoscopic Ultrasound

(LUS)) was reported in [4-8]. Minimally invasive procedure requires precise tracking and hand eye calibration because of limited view of camera where image may need to be magnified for better interpretation of anatomy [9]. The calibration using optical tracking in proximal end is prone to large tracking error compared to using Electromagnetic Sensor (EMS) near the camera [4], [8-9]. Furthermore, hand eye calibration requires at least two distinct motions with non-parallel rotation axes. The transformation cannot be obtained if there exist limiting cases such as pure translation or rotation.

In order to calculate optimum transformation parameters, [3,10-13] implemented linear least square algorithm with OTS as main reference frame. The calibration in [3,10,12,13] were limited to rigid surgical device while MIS require frequent use of flexible surgical device. As the whole distortion correction was based on OTS, the magnetic distortion correction mechanism may provide false correction vector even if Line of Sight (LOS) is blocked for few seconds accidentally for real time and preoperative correction mechanism [3], [11-13]. Furthermore, the system was modeled for static distortion [3,11,12]. Hence, the correction vector would be redundant if the distortion in the vicinity of EMTS changes during surgery.

The Levenberg-Marquardt, iterative method to solve nonlinear least squares problems by minimizing the cost function, was implemented for calibration of LUS probe with tracking devices [4-6], [11], [14-16]. Levenberg-Marquardt algorithm suffers from two complementary problems: slow convergence and robustness to initial guess [17]. Method implemented to increase the convergence speed yield decreased robustness to the initial guess. Hence user needs to manually adjust the algorithm parameters according to the particular requirement [17].

Researchers in [18-19] performed fiducial marker/landmark-based calibration between preoperative CT with the tracking device by using Horn's absolute orientation method [20]. The work of [19] provided the contextual information for localizing targets for novice and experienced surgeon. However, the high precision task such as needle placement, ablation require higher accuracy; ultrasound probe itself has tendency to distort the EM tracking measurement. On the other hand, the evaluated accuracy of 24.17mm in [19] is not acceptable for clinical application.

Researchers in [21] presented the calibration of LRS with OTS. Same fiducial markers were extracted in both coordinate frames for calibration. In addition to requirement of constant line of sight, performance of OTS is widely affected by various lighting condition in room. Furthermore, the optical markers located at handle of surgical pointer require additional fixed transformation between the optical makers and surgical pointer tip. This may induce additional error in the system.

Existing calibration systems use the fusion of Optical Tracking System (OTS) and/or EMTS with intraoperative image such as endoscope, Laparoscopic Ultrasound System (LUS), and preoperative CT/MRI image [3-6], [8], [11,15,19]. OTS becomes redundant in scenario crowded with medical device and surgeon in incision-based MIS approach[22]. Ultrasound suffers from shadowing, multiple reflections, low signal to noise ratio, requirement of expertise and training of surgeon. The use of ultrasound within the EMTS field is also responsible for added distortion in EMTS measurement [22]. While implementing two heterogeneous sensors, researchers have fused information from intraoperative images (LUS/Endoscope/DynaCT) with preoperative images (CT/MRI) [23] or with navigation system (EMTS/OTS), [1,8,10,14,24-26]. The information gathered from two sensors is not sufficient for performing successful MIS.

In order to perform successful MIS, one needs at least three heterogeneous sensors: at least two for preoperative and intraoperative imaging, and one for navigation purpose. The combination of these three heterogeneous sensors provides sufficient information for real time visualization, positional information of the surgical tools, and real time path planning. This paper presents our offline spatial calibration among three heterogeneous sensors. The proposed hybrid system involves EMTS, videoscope, and LRS. In addition to not requiring the LOS, the EMS can be directly inserted to the point of interest without surgical pointer. To the best of our knowledge this is first approach of offline calibration of three heterogeneous sensors which involve LRS, EMTS, and Camera together. LRS is used here to emulate CT/MRI preoperative data, camera for real time high quality images, and EMTS for positional information inside the human body. EMTS is the best method of tracking in MIS approaches where line of sight is not available [27]. Up to now no universally acceptable alternative of EMTS has been developed [27].

Each of three heterogeneous sensors used in this work have their own coordinate frame and data rates. To provide the surgeon with useful real time video and positional information of the surgical tool(s), all the sensors data have to be represented in the same coordinate frame with proper synchronization. Hence the calibration process may be classified as problem of spatiotemporal calibration. Off-line calibration is a pre-requisite for real time tracking, once the time synchronization problem is resolved. Hence, we have considered temporal calibration of asynchronous sensors and their real-time tracking as future work.

This paper is organized as follows. Section II discusses the hardware used to perform the calibration and experimental testing. Section III discusses the proposed calibration technique and its justification. Section IV discusses the accuracy obtained using the proposed calibration technique. Section V contains conclusions and discusses future work.

Hybrid Tracking Hardware

LRS from Next Engine was used as 3D scanner to imitate the preoperative CT/MRI machine. The LRS consists of four scanning lasers with scanning resolution of 500 DPI (Dots per Inch) in macro mode and 200 DPI in wide mode [28]. The images from each scanning lasers were processed and fused to give the xyz position and RGB value of a pixel in the LRS coordinate frame. The navigation sensor used was NDI Type-2 6DOF sensor for Aurora EMTS with measurement frequency of 40Hz [29]. It provides position and orientation information in reference to tabletop field generator. According to NDI, the accuracy is 0.8 mm for position and 0.7degree for orientation for EMTS measurement [29]. The third sensor was the Go 5000C series color camera from JAI Corporation [30], with 5-mega-pixel resolution.

Proposed Calibration Technique

The implementation of multimodal display including tracked

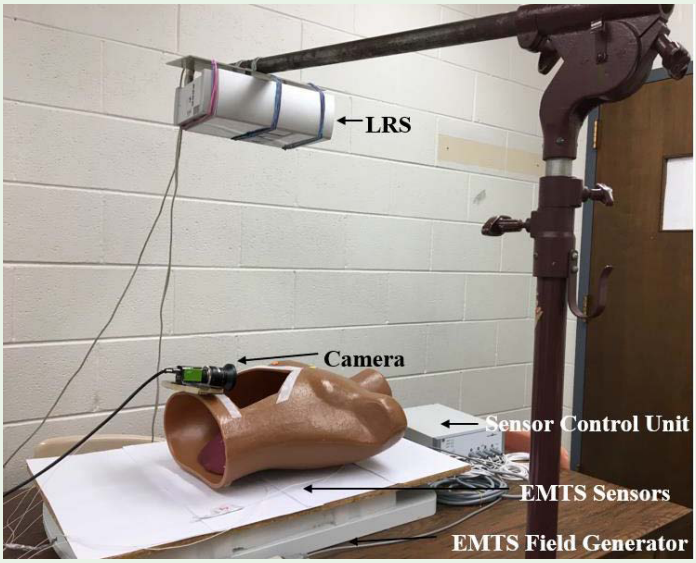

Figure 1: Heterogeneous sensors for proposed system. EMTS is the tracking system; Camera is for intraoperative while LRS is for preoperative imaging.

videoscope along with preoperative data can be potentially helpful to detect and correct possible anatomical shifts. The videoscope data will provide updated information that the surgeon can rely on, while he/she can also benefit from preoperative data with real time view and understanding of anatomy. We have selected LRS as the standard reference frame. Figure 1 and 2(a) show all the coordinate systems involved and the coordinate transformation among them. Registering the data in preoperative images as the absolute coordinate frame allows precise advanced AR visualization as well as therapy delivery [31]. The camera itself consists three coordinate systems as shown in Figure 2(b): 3D camera focal point coordinates, 2D coordinates of the center of the image plane, and 2D coordinates of the origin of the camera image. The depth information is lost during transformation of focal point to image plane coordinate system.

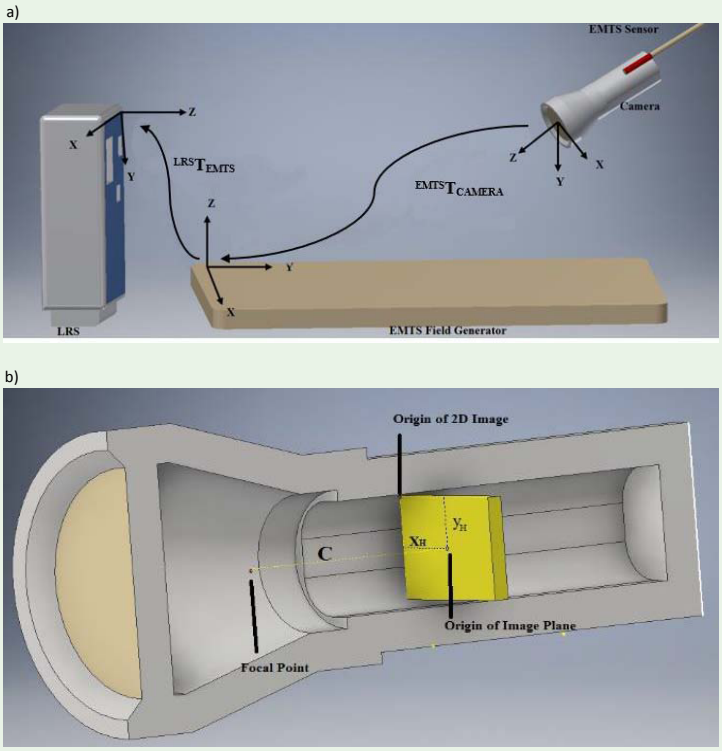

Figure 2: (a) Transformation among the different coordinate systems involved. (b) Three coordinate systems (Focal point, Origin of 2D image, Origin of image plane) involved in camera.

The selected calibration object involves two planes and each plane with four circular patterns of different colors (Blue, Pink, Red, Purple), Figure 3 [32]. The design of the calibration object satisfies the requirement of Direct Linear Transform (DLT) camera calibration: at least six calibration points located in different planes [33]. The idea of using different color for calibration objects is to simplify the calibration point extraction for LRS and camera coordinate frame by using a color filter algorithm. This work advances the work of [32] toward spatiotemporally calibration of three heterogeneous sensors which are necessary for real time visualization and navigation to perform successful MIS.

Let us consider the surgeon needs to identify and reach the target area in minimally invasive fashion. Preoperative imaging provides 3D overview of patient. Surgeon can rely on these high-quality 3D images to diagnose the problem inside body. When the target anatomy is recognized, the same preoperative images can be used for 3D path planning to reach the destination with shortest path facing the minimum obstacle. As there exists fixed transformation between EMTS and CT/MRI reference frames, every point along with the planned path can be recognized in CT/MRI coordinate frame. Once the position of camera, planned path, and the destination point all are in CT/MRI coordinate frame, surgical tool can be driven to destination correctly with real time feedback from EMS attached to the camera. Once the destination is reached, the target anatomy in CT/MRI can be segmented to extract relevant features such that the 2D camera image can be overlaid on the top of 3D image for augmented view within human body.

Calibration Point Extraction in LRS and EMTS Coordinate Frame

In order to obtain the eight calibration points in LRS coordinate frame, the calibration device was scanned with ScanStudio HD. The point cloud was preprocessed to remove any unnecessary artifacts; Figure 4(a) after preprocessing the point cloud was fed to an algorithm to extract the eight calibration points. The algorithm works as follows

1. Extract calibration points in four bins according to their RGB color range. Each bin will contain set of position and RGB value of two circular patterns of same color but located at front and black plane.
2. Determine the centroid along the z axis of point cloud. Z axis centroid acts as reference between two planes.
3. Transfer the calibration points in four bins to eight bins with reference to the centroid along the z axis.
4. Remove any outlier pointed detected beyond the 5mm radius of circular pattern each circular pattern has radius of 5mm. Any point that is detected beyond that range is falsely detected point and should be removed.
5. Finally, calculate eight calibration points (red dots) in LRS frame, Figure 4(b).

3-D coordinate of calibration point in EMTS were acquired by inserting the EMS at the center of each circular patterns in predefined order.

Calibration Point Extraction in Camera Coordinate Frame

In order to extract calibration points in camera coordinate frame, an image processing algorithm was developed. The algorithm performs morphological image processing [34] and removes any background objects in the field of view of camera.

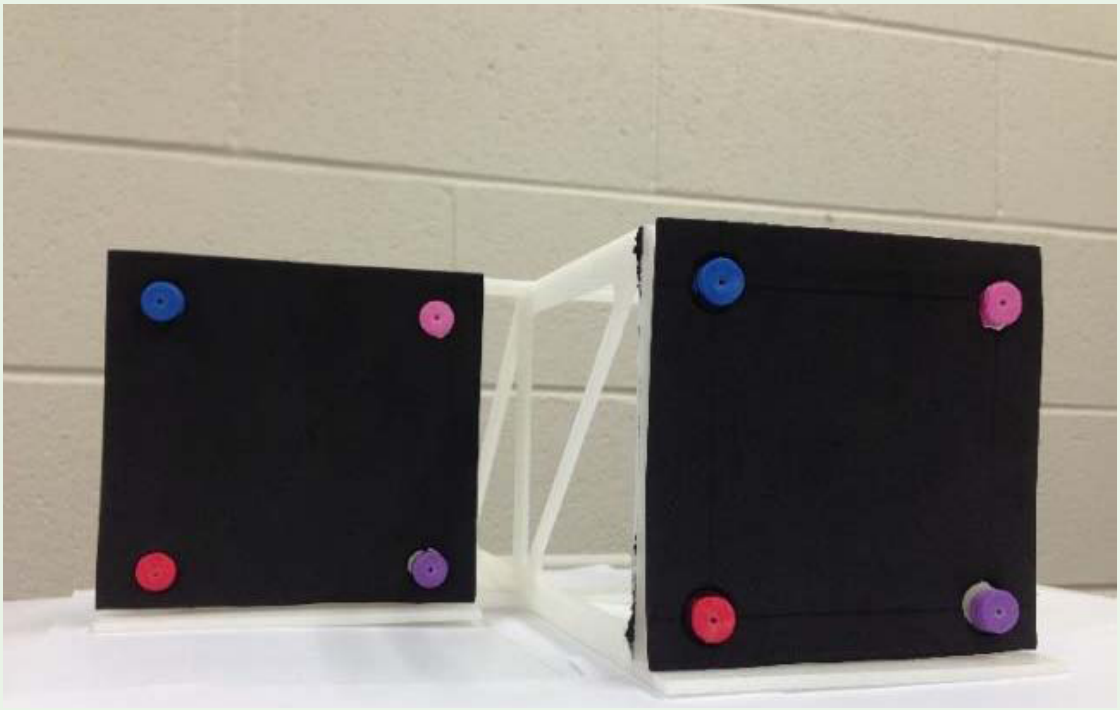

Figure 3: Calibrations object with two planes. Blue, Pink, Red, and Purple calibration objects of radius 5mm are attached in each plane of the device.

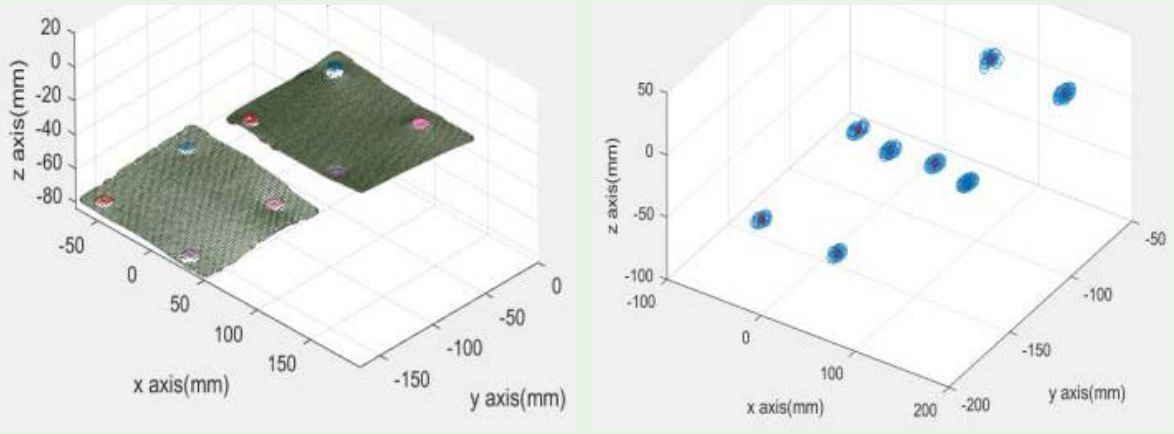

Figure 4: (a) 3D point cloud of calibration object after preprocessing (b) Extraction of calibration points in LRS coordinate frame. Red points, hidden within blue circles, indicate the calibration points.

The next step is to extract the calibration points and arrange them in specific order. Before calculation of centroids of each connected component, one needs to label them first. During connected component labeling, Image processing toolbox scans objects from top to bottom starting from the leftmost position and ending at rightmost position. This labelling may change according to different position from where the image is taken. In order to solve this problem, the labeled connected components were first arranged as top and bottom components in image. Later the arranged connected components were rearranged in order on the basis of their presence in front and back plane of the calibration object. Once we order the labeling of connected component, we can calculate the calibration points, Figure 5.

In order to calibrate LRS with EMTS, Horn's absolute orientation method based on unit quaternion was implemented [20].

In addition, we implemented Direct Linear Transform (DLT) for camera calibration. Horn's quaternion-based approach and DLT method both provide closed form solution [20,33]. Both approaches are computationally efficient as they are not iterative. Iterative approaches have tendency to end up in local minima unless a good initial approximation provided. Horn's method provides the efficient solution compared to training based Artificial Neural Network (ANN), Genetic algorithm [32].

The DLT camera calibration can be done by using single image of calibration object unlike planar pattern which require image of at least two different orientations of the object [35]. The process is less prone to error because it doesn't require additional hand-eye calibration to transform camera position and orientation in planar pattern to the EMTS coordinate frame.

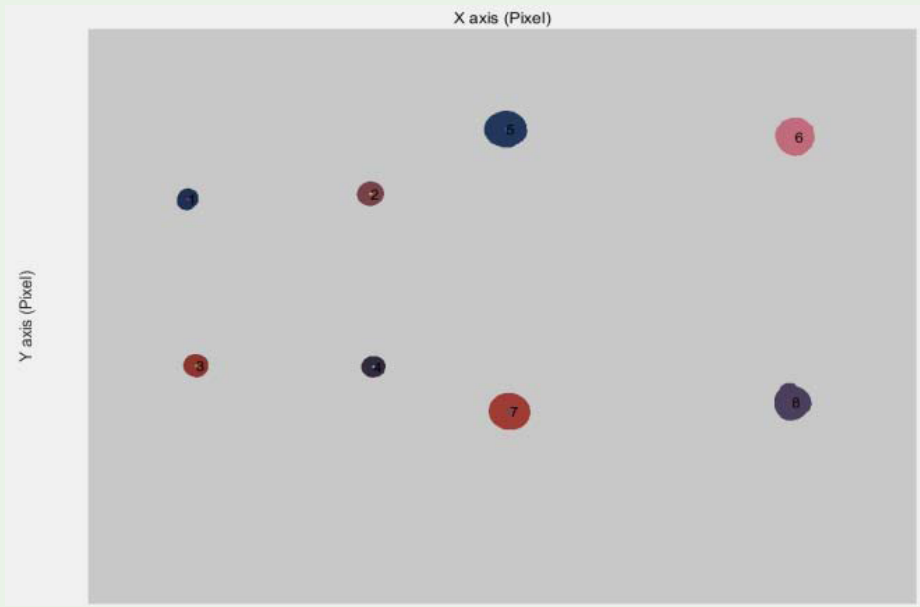

Figure 5: Extraction of calibration points in camera image. Labelling from 1 to 8 indicate the calibration points and their measurement order.

Spatial Calibration between LRS and EMTS

The problem of coordinate transformation between LRS and EMTS consists of finding rotation and translation matrices using positional information of the same entity measured by the two sensors in their local reference frame. If *P*EMTS is a 3D point in EMTS coordinate frame, it can be transferred to LRS coordinate frame as

$$p_{\text{LRS}} = RP_{\text{EMTS}} + \text{T} \quad (1)$$

Where, PLRS is the transformed EMTS point in LRS coordinate frame, *R* is rotation matrix and *T* is translation vector. The transformation can be determined with three perfect non-collinear calibration points [20]. Including more points for calibration leads to over determined system with increased accuracy [20]. Maximum accuracy of transformation between LRS and EMTS is achieved by using eight calibration points.

Pseudo code for Horn's Absolute Orientation for transformation from LRS to EMTS.

1. Inputs: Calibration point in LRS (*PLRS*) and EMTS - (*PEMTS*).
2. Compute: *CLRS* =Centroid of PLRS and CEMTS =centroid of *PEMTS*
3. Calculate: $A = P_{LRS} - C_{LRS}$, $B = P_{EMTS} - C_{EMTS}$
4. Calculate M = A*B^{T}, Such that

$$M = \begin{bmatrix} s_{xx} s_{xy} s_{xz} \\ s_{yx} s_{yy} s_{yz} \\ s_{zx} s_{zy} s_{zz} \end{bmatrix}$$

5. Calculate

$$N = \begin{bmatrix} s_{xx} + s_{yy} + s_{zz} & s_{yz} - s_{ZY} & s_{zX} - s_{xz} & s_{XY} - s_{yX} \\ s_{yz} - s_{zy} & s_{xx} - s_{yy} - s_{zz} & s_{XY} + s_{YX} & s_{zx} + s_{xz} \\ s_{zx} - s_{xz} & s_{XY} + s_{YX} & -s_{xx} + s_{yy} - s_{zz} & s_{yz} + s_{ZY} \\ s_{xy} - s_{yx} & s_{zx} + s_{xz} & s_{yz} + s_{ZY} & -s_{xx} - s_{yy} + s_{zz} \end{bmatrix}$$

6. λmax = Most positive Eigen Value of N
7. ν max = Eigen Vector Corresponding to λmax
8. Normalize ν max to get unit quaternion representation of rotation $q=q_o + iq_{x+} jq_{y+} kq_z$
9. Calculate

$$R = \begin{bmatrix} q_o^2 + q_x^2 - q_y^2 - q_z^2 & 2(q_x q_y - q_o q_z) & 2(q_x q_z + q_o q_y) \\ 2(q_x q_y - q_o q_z) & q_o^2 - q_x^2 + q_y^2 - q_z^2 & 2(q_y q_z + q_o q_x) \\ 2(q_x q_z - q_o q_y) & 2(q_y q_z + q_o q_x) & q_o^2 - q_x^2 + q_y^2 - q_z^2 \end{bmatrix}$$

10. T=C_{MTS}-RC_{LRS}

Spatial Calibration between EMTS and Camera

Normalized DLT maps any point in world coordinate system to the camera coordinate system. Data normalization involves the translation and scaling of calibration points and it should be carried out before implementation of DLT algorithm [33]. Apart from improved accuracy in result, the result of data normalization will be invariant with respect to the arbitrary choices of scale and coordinate origin [33]. The matrix *M* in equation (2) has eleven unknown parameters. In order to determine the unique solution of these parameters, we need at least 6 points, and all of them should not lie in same plane [33]. Let us consider a point *P* in EMTS coordinate system is to be transformed to camera sensor coordinate system *p* both in homogeneous form.

$$P_{3\chi 1} = K_{3\chi 3} R_{3\chi 3} \left[I_{3\chi 3} \middle| -X_{0_{3\chi 1}} \right] P_{4\chi 1} = M_{3\chi 4} X_{4\chi 1} \quad (2)$$

Where, *K*: 3 x 3 camera intrinsic parameter matrix: consists 5 intrinsic parameters: camera constant(*c*), scale difference(*m*), sheer component (*s*), transformation between plane coordinate system to sensor coordinate system (*xH, yH*); *R*: 3 x 3 rotation matrix; *X0* : 3 x 1 translation vector; *I:* 3 x 3 identity matrix.

Pseudocode for DLT

1. Inputs: camera image coordinate (p_{cam}) and EMTS coordinate (P_{EMTS})(i≥6)
2. $\overline{P}_{cam}$ = mean (p_{cam}), $\overline{P}_{EMTS}$ = mean (P_{EMTS})
3. Shift origin of camera and EMTS data to $\overline{P}_{cam}, \overline{P}_{EMTS}$
4. $[\text{pn} \quad \text{pn}] = \text{Normalize}\left(\overline{P}_{cam}, \overline{P}_{EMTS}\right)$
5. Calculate Homography(M)

$$M = \begin{bmatrix} -X_{n_i} & -Y_{n_i} & -Z_{n_i} & -1 & 0 & 0 & 0 & 0 & x_{n_i} X_{n_i} & x_{n_i} Y_{n_i} & x_{n_i} Z_{n_i} & x_{n_i} \\ 0 & 0 & 0 & 0 & -X_{n_i} & -Y_{n_i} & -Z_{n_i} & -1 & y_{n_i} X_{n_i} & y_{n_i} Y_{n_i} & y_{n_i} Z_{n_i} & x_{n_i} \end{bmatrix}_{2ix12}$$

6. [U S V] =SVD (M)
7. Select eigen vector (ν) corresponding to smallest singular value which minimizes error

8. Renormalize and Rearrange (ν)

9. [R,K]=QR_decomp(ν)

10. [X_o]=camcenter(ν)

Experimental Performance Evaluation

In order to assess the accuracy of the proposed calibration, ten colored circular objects were attached to the surface of an artificial liver available in lab, Figure 6(a). The centroids were acquired by the LRS, EMTS, and Camera in their respective frames. These circular objects can represent presence of liver tumor. In LRS coordinate frame, the colored objects were first extracted on the basis of color filter algorithm, Figure 6(b). In camera coordinate system the image was fed to image processing algorithm to remove background, clear

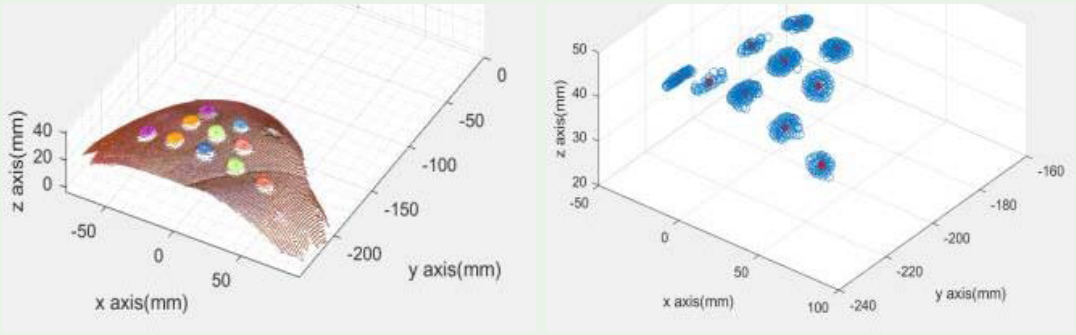

Figure 6: (a) 3D point cloud of artificial liver after preprocessing in Scan Studio. (b) Extraction of accuracy evaluation in LRS coordinate frame. Red points indicate the extracted points (c) Extraction of accuracy evaluation point in camera frame.

border, clear holes, and label and arrange the connected components, and determine the centroid of each connected component, Figure 6(c). EMTS data were acquired by inserting the EMS in colored object.

The calculated centroid from LRS frame was first transformed to EMTS coordinate frame according to calibration parameter, equation (3). The performances of two rigid registration algorithms for LRS to EMTS transformation were compared for accuracy evaluation: algorithm proposed by Horn, and the algorithm proposed by Walker et al. [36]. The calibration and accuracy evaluation were performed in environment without any ferromagnetic material near the EM field generator. Tracking in the electromagnetic field generator is unaffected by the medical-grade stainless steel (300 series), titanium, and aluminum [22,29]. The tabletop field generator also minimizes distortions produced from the patient table or materials located below it [29]. Once the set of points were transformed from LRS to EMTS they were projected to distortion corrected camera image, equation (4). We have tested the accuracy of the calibration for the liver shown in Figure 6(a) for ten different arrangements. Accuracy was evaluated at least 12inch from the top surface of EMTS field generator so as to provide room for placement of patient table.

$$ {}^{EMTS}X_{LRS} = {}^{EMTS}T_{LRS} \bullet X_{LRS} \tag{3} $$

$$ \begin{bmatrix} {}^{CAM}X_{LRS} \\ 1 \end{bmatrix} = {}^{CAM}T_{EMTS} \begin{bmatrix} {}^{EMTS}X_{LRS} \\ 1 \end{bmatrix} \tag{4} $$

In equation (3) and (4), ${}^{A}T_{B}$ represents the transformation parameter from coordinate system B to coordinate system A, while ${}^{A}X_{B}$ represents the transformed point from B to A.

Figure 7(a) illustrates the registration error in each axis for LRS to EMTS transformation. As both algorithms provide the closed form solution, the average error difference is within millimeter range

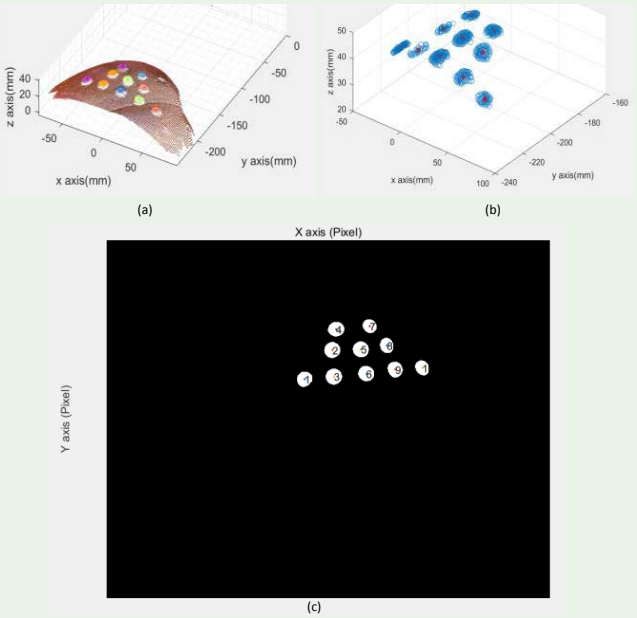

Figure 7: (a) Error of Transformation from LRS to EMTS using Horn's method and Walker's method. (b) Error of transformation from transformed LRS points to 2D camera image.

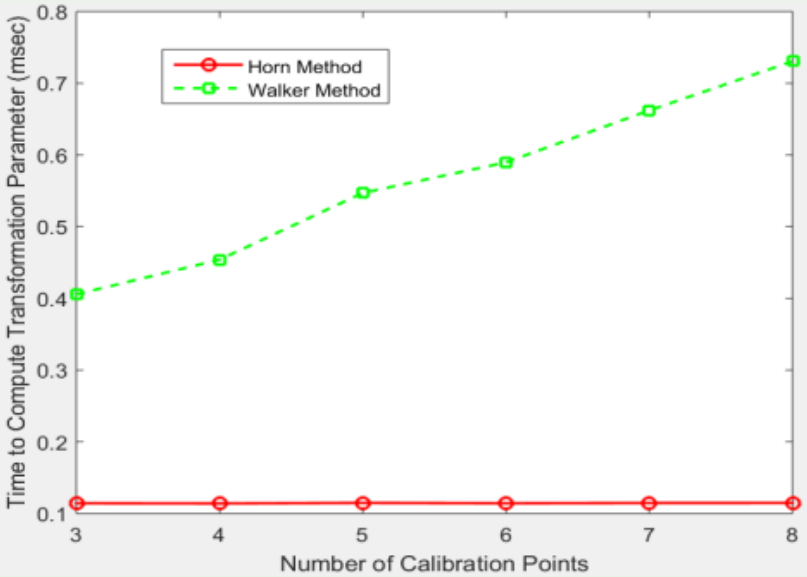

Figure 8: Computation Time vs Number for Calibration Points [20], [36].

for LRS to camera coordinate frame, Figure 7(b). In addition to the accuracy evaluation, the computation time of each algorithm was compared. Both algorithms in [20] and [36] require at least three calibration points spatially located at same place. The computation time for the algorithm proposed by Walker et al. increases drastically compared to the almost constant computation time for the Horn's method with increasing number of calibration points, Figure 8.

Table I summarizes the absolute positional error for coordinate transformation from LRS to EMTS as well as EMTS to camera frame using Horn's, and DLT method respectively. The average error for LRS to EMTS coordinate transformation is minimum along Z axis. The Y coordinate seems to be most affected by error with maximum standard deviation and range. The X and Z coordinate provide more consistent reading compared to largely fluctuating Y coordinate values, Figure 7(a). There might be two possible reasons for the error.

First reason may be the varying ability of LRS to correctly scan and replicate the scanned object at varying distance. According to Feng *et al.* [37] the signal attenuation increases with increase in the distance of scanned surface from LRS. This reduces the ability of scanner to correctly localize the point cloud. If Figure 4(a) is closely observed there are two separate planes along the Z axis of calibration device at the increasing distance from the scan position of LRS. The Z coordinate in LRS might be transformed to the Y coordinate of EMTS during coordinate transformation. The second reason may be due to error in data collection.

In order to correctly scan an object, the laser beam should be normal to the surface to be scanned [37]. Considering the shape of the scanned liver it might be possible that some surfaces were not perfectly normal to the laser beam and contributed for the system error. Ten experiments were performed to measure the registration error of the two-plane calibration device by moving it to another position. The total registration error was 0.5862± 0.3901mm, 1.1255±0.5850mm, 0.5815±0.4440mm along the x, y, and z direction respectively. The result supports the claim proposed by [37]. Furthermore, the capability to accuracy measure the data with each measurement system also affects the overall error of the hybrid system. For instance, the accuracy in measurement of EMTS is 0.8 mm for position and 0.7degree for orientation as reported by NDI.

EMTS to camera transformation error is the overall error associated with the hybrid tracking system because the evaluated error is the integrated error from the LRS to EMTS and EMTS to camera transformation, Table I. Although the error is within millimeter range, it is mainly due to propagation of error generated during LRS to EMTS coordinate transformation. The propagation of error from one coordinate transformation to another is the main disadvantages of the hybrid tracking system.

RS Jose [19] calibrated OTS with CT scan using Horn's absolute orientation method with reported overall system error of 24.17mm. In addition to Fiducial Registration Error (FRE), the transformation error between the optical marker and the surgical pointer contributed the poor performance of the system [19]. Our system is immune to the possible registration error between the optical marker and surgical pointer because of direct insertion of EMS coils to the point of interest. Furthermore, our result shows that the EMTS can work as the efficient localization device under non-ferromagnetic condition. This result is also an improvement over the distortion corrected average accuracy of 2.1±0.8 mm for OTS and EMTS calibration reported in [12].

Table 1: Absolute Error Analysis of Transformation from Lrs to Emts to 2d Image (Horn's Method).

	LRS to EMTS			EMTS to Image	
	X	Y	Z	X	Y
Mean(mm)	1.3511	2.6019	1.1325	0.1081	0.0872
S. D.(mm)	0.9321	1.5239	0.9285	0.0606	0.0298
Range(mm)	4.1423	7.0469	4.2079	0.1802	0.0879

Conclusion and Future Work

This paper provided a first step toward building a platform for using a set of asynchronous sensors so to make safe navigation inside the human body possible. The LRS is used in this paper to provide the preoperative information that would be given by a CT/MRI in a hospital setting. However, the registration process is still applicable when CT/MRI is used. Furthermore, for laboratory testing, a low cost 2D camera is used. The proposed technique applies to any camera as long as the specific parameters of the camera are provided to the registration algorithm.

Laboratory testing using an artificial liver was carried out which showed promising accuracy.

Future work will extend the result of this paper to include temporal and spatial registration of asynchronous heterogeneous sensors. The next phase is necessary because in addition to having data in different spatial coordinate frames, the heterogeneous sensors have different data rate based on independent clocks.

References

1. Thoranaghatte RU, Zheng G, Langlotz F, Nolte LP. Endoscope-based hybrid navigation system for minimally invasive ventral spine surgeries. Comput Aided Surg 2005; 10: 351-356.
2. Peters T, Cleary K. Image-Guided Interventions: Technology and Applications. Springer Science and Business Media 2008.
3. Nakada K, Nakamoto M, Sato Y, Konishi K, Hashizume M, Tamura S. A rapid method for magnetic tracker calibration using a magneto-optic hybrid tracker. International Conference on Medical Image Computing and Computer-Assisted Intervention 2003; 2879: 285-293.
4. Feuerstein M, Reichl T, Vogel J, Traub J, Navab N. Magneto-optical tracking of flexible laparoscopic ultrasound: model-based online detection and correction of magnetic tracking errors. IEEE Trans Med Imaging 2009; 28: 951-967.
5. Nakada K, Nakamoto M, Sato Y, Konishi K, Hashizume M, Tamura S. Intraoperative magnetic tracker calibration using a magneto-optic hybrid tracker for 3-D ultrasound-based navigation in laparoscopic surgery. IEEE Trans Med Imaging 2008; 27: 255-270.
6. Fakhfakh HE, Llort-Pujol G, Hamitouche C, Stindel E. Automatic registration of pre-and intraoperative data for long bones in minimally invasive surgery. Conf Proc IEEE Eng Med Biol Soc 2014; 2014: 5575-5578.
7. Martens V, Schlichting S, Besirevic A, Kleemann M. LapAssistent—a laparoscopic liver surgery assistance system. IFMBE Proceedings 2009; 22: 121-125.
8. Wengert C, Bossard L, Häberling A, Baur C, Székely G, Cattin PC. Endoscopic navigation for minimally invasive suturing. Med Image Comput Comput Assist Interv 2007; 10: 620-627.
9. Thompson S, Stoyanov D, Schneider C, Gurusamy K, Ourselin S, Davidson B, et al. Hand-eye calibration for rigid laparoscopes using an invariant point. Int J Comput Assist Radiol Surg 2016; 11: 1071-1080.
10. O. V. Solberg, T. Langø, G. A. Tangen, R. Mårvik, B. Ystgaard, A. Rethy et al. Navigated ultrasound in laparoscopic surgery. Minimally Invasive Therapy & Allied Technologies 2009; 18: 36-53.
11. Konishi K, Nakamoto M, Kakeji Y, Tanoue K, Kawanaka H,Yamaguchi S, et al. A real-time navigation system for laparoscopic surgery based on three-dimensional ultrasound using magneto-optic hybrid tracking configuration. Int J CARS 2007; 2: 1-10.
12. Birkfellner W, Watzinger F, Wanschitz F, Ewers R, Bergmann H. Calibration of tracking systems in a surgical environment. IEEE Trans Med Imaging 1998; 17: 737-742.
13. Nakamoto M,Sato Y, Tamaki Y,Nagano H, Miyamoto M, Sasama T, et al. Magneto-optic hybrid 3-D sensor for surgical navigation. MICCAI 2000; 1935: 839-848.
14. Prager RW, Rohling RN, Gee AH, Berman L. Rapid calibration for 3-D freehand ultrasound. Ultrasound Med Biol 1998; 24: 855-869.
15. Sato Y, Nakamoto M, Tamaki Y, Sasama T, Sakita I, Nakajima Y, et al. Image guidance of breast cancer surgery using 3-D ultrasound images and augmented reality visualization. IEEE Trans Med Imaging 1998; 17: 681-693.
16. J. Chaoui, G. Dardenne, C. Hamitouche, E. Stindel, C. Roux. Virtual movements-based calibration method of ultrasound probe for computer assisted surgery. IEEE International Symposium on Biomedical Imaging: From Nano to Macro, Boston 2009; 2009: 1207-1210.
17. Transtrum MK, Sethna JP. Improvements to the Levenberg-Marquardt algorithm for nonlinear least-squares minimization. arXiv 2012; 1201: 5885.
18. Pyciński B, Juszczyk J, Bożek P, Ciekalski J, Dzielicki J, Pietka E. Image navigation in minimally invasive surgery. Information Technologies in Biomedicine 2014; 4: 25-34.
19. Estépar RS, Stylopoulos N, Ellis R, Samset E, Westin CF, Thompson C, et al. Towards scarless surgery: an endoscopic ultrasound navigation system for transgastric access procedures. Comput Aided Surg 2007; 12: 311-324.
20. Horn BK. Closed-form solution of absolute orientation using unit quaternions. J Opt Soc Am A 1987; 4: 629-642.
21. Cash DM, Sinha TK, Chapman WC, Terawaki H, Dawant BM, Galloway RL, et al. Incorporation of a laser range scanner into image-guided liver surgery: surface acquisition, registration, and tracking. Med Phys 2003; 30: 1671-1682.
22. Birkfellner W, Hummel J, Wilson E, Cleary K. Tracking devices. in Image-Guided Interventions 2008; 23-44.
23. Marami B, Sirouspour S, Fenster A, Capson DW. Dynamic tracking of a deformable tissue based on 3d-2d mr-us image registration. SPIE Medical Imaging 2014; 9036: 90360T.
24. Sindram D, McKillop IH, Martinie JB, Iannitti DA. Novel 3-D laparoscopic magnetic ultrasound image guidance for lesion targeting. HPB (Oxford) 2010; 12: 709-716.
25. Mercier L, Langø T, Lindseth F, Collins DL. A review of calibration techniques for freehand 3-D ultrasound systems. Ultrasound Med Biol 2005; 31: 143-165.
26. Ng CS, Yu SC, Lau RW, Yim AP. Hybrid DynaCT-guided electromagnetic navigational bronchoscopic biopsy. Euro J Cardiothoracic Surg 2015; 49: i87-i88.
27. Franz AM, Haidegger T, Birkfellner W, Cleary K, Peters TM, Maier-Hein L. Electromagnetic tracking in medicine-a review of technology, validation, and applications. IEEE Trans Med Imaging 2014; 33: 1702-1725.
28. NextEngine 3D Laser Scanner
29. Aurora
30. GO-5000M-USB / GO-5000C-USB.
31. Sauer F. Image registration: Enabling technology for image guided surgery and therapy. Conf Proc IEEE Eng Med Biol Soc 2005; 7: 7242-7245.
32. Ruehling DE. Development and Testing of a Hybrid Medical Tracking System for Surgical Use. MS Thesis, Tennessee Technological University, Cookeville, 2015.
33. Hartley R, Zisserman A. Multiple View Geometry in Computer Vision. 2003.
34. Gonzalez RC, Woods RE. Digital image processing. 2012.
35. Camera Calibration Toolbox for Matlab.
36. Walker MW, Shao L, Volz RA. Estimating 3-D location parameters using dual number quaternions. CVGIP: Image Understanding 1991; 54: 358-367.
37. Feng H, Liu Y, Xi F. Analysis of digitizing errors of a laser scanning system. Precision Engineering 2001; 25: 185-191.